Biology of Reproduction, 2021, 105(2), 491–502
https://doi.org/10.1093/biolre/ioab083
Research Article
Advance Access Publication Date: 28 April 2021

Research Article

MAP3K4 kinase activity dependent control of mouse gonadal sex determination†

Noha A.M. Shendy[1,2], Amber L. Broadhurst[1], Kristin Shoemaker[1], Robert Read[1] and Amy N. Abell[1,*]

[1]Department of Biological Sciences, University of Memphis, Memphis, TN, USA and [2]Department of Chemistry, Faculty of Science, Mansoura University, Mansoura, Egypt

***Correspondence:** Department of Biological Sciences, University of Memphis, Memphis, TN 38152, USA.
E-mail: anabell@memphis.edu

†Grant Support: This research was supported by the National Institutes of Health General Medical Sciences (Grant GM116903) and by the Memphis Research Consortium to A.N.A.

Received 15 September 2020; Revised 22 February 2021; Accepted 21 April 2021

Abstract

Sex determination requires the commitment of bipotential gonads to either a testis or an ovarian fate. Gene deletion of the kinase *Map3k4* results in gonadal sex reversal in XY mice, and transgenic re-expression of *Map3k4* rescues the sex reversal phenotype. *Map3k4* encodes a large, multi-functional protein possessing a kinase domain and several, additional protein–protein interaction domains. Although MAP3K4 plays a critical role in male gonadal sex determination, it is unknown if the kinase activity of MAP3K4 is required. Here, we use mice expressing full-length, kinase-inactive MAP3K4 from the endogenous *Map3k4* locus to examine the requirement of MAP3K4 kinase activity in sex determination. Although homozygous kinase-inactivation of MAP3K4 ($Map3k4^{KI/KI}$) is lethal, a small fraction survive to adulthood. We show $Map3k4^{KI/KI}$ adults exhibit a 4:1 female-biased sex ratio. Many adult $Map3k4^{KI/KI}$ phenotypic females have a Y chromosome. XY $Map3k4^{KI/KI}$ adults with sex reversal display female mating behavior, but do not give rise to offspring. Reproductive organs are overtly female, but there is a broad spectrum of ovarian phenotypes, including ovarian absence, primitive ovaries, reduced ovarian size, and ovaries having follicles in all stages of development. Further, XY $Map3k4^{KI/KI}$ adults are smaller than either male or female $Map3k4^{WT/WT}$ mice. Examination of the critical stage of gonadal sex determination at E11.5 shows that loss of MAP3K4 kinase activity results in the loss of *Sry* expression in XY $Map3k4^{KI/KI}$ embryos, indicating embryonic male gonadal sex reversal. Together, these findings demonstrate the essential role for kinase activity of MAP3K4 in male gonadal sex determination.

Summary sentence

Male gonadal sex determination requires the kinase activity of the multi-domain containing protein MAP3K4.

Graphical Abstract

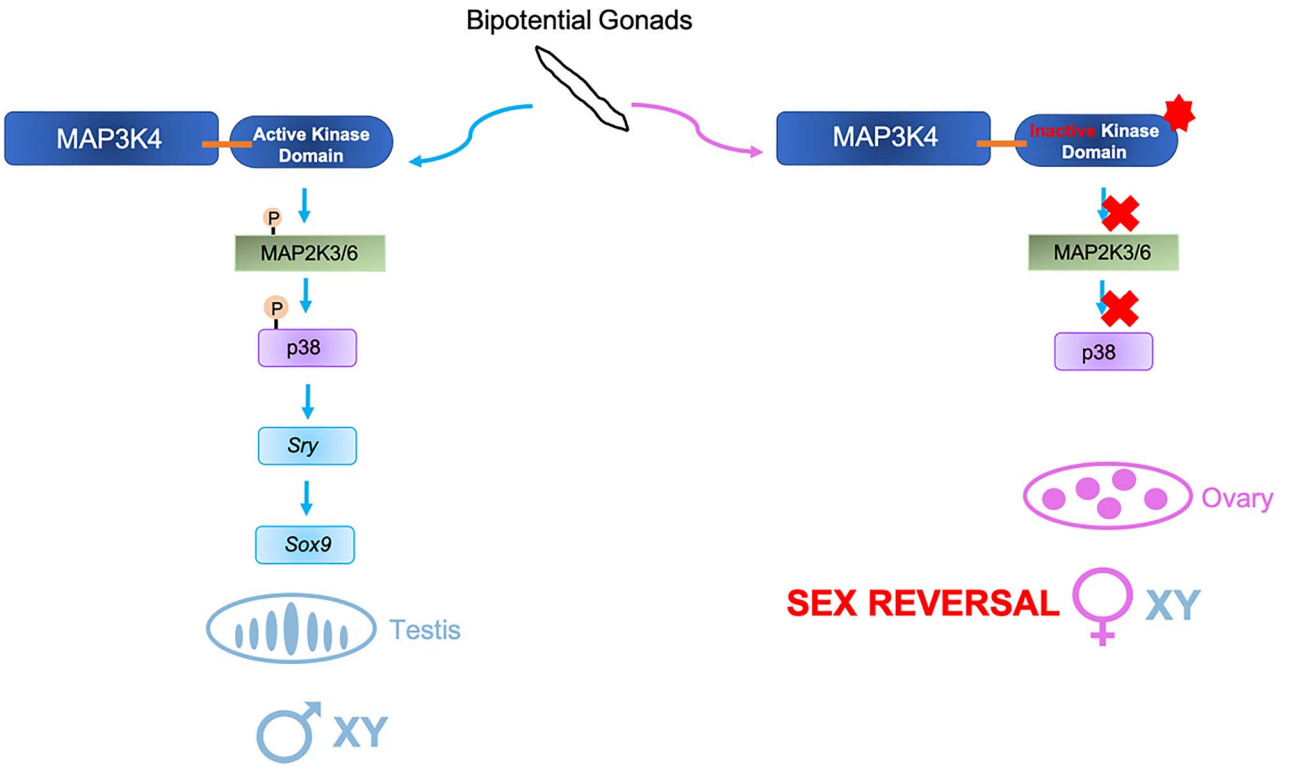

Key words: gonadal sex determination, kinase activity, MAP3K4, mitogen-activated protein kinase kinase kinase 4, MAP2K3/6, p38 MAPK, SRY.

Introduction

The decision of mammalian bipotential gonads to differentiate into ovaries or testes is controlled by the process of gonadal sex determination [1–3]. In XY individuals, the expression of the Y-linked gene *Sry* triggers pathways that support the differentiation of the bipotential gonads into the testes [4]. Absence of the *Sry* gene in XX individuals allows the initiation of the mutually antagonistic female developmental pathways [5–7]. Disturbances in molecular pathways controlling sex determination can result in a sex reversal phenotype where the sexual phenotype does not match the genetic sex [2, 3]. For example, XY individuals can develop ovaries and a female phenotype.

Previous studies have defined the essential role of the mitogen-activated protein kinase (MAPK) signaling cascade during mouse gonadal sex determination [2, 8–11]. MAPK signaling pathways are evolutionarily conserved and modulate diverse cellular processes, including survival, proliferation, differentiation, and inflammation [12]. These pathways are activated in response to a wide range of extracellular stimuli such as mitogens and cellular stresses. MAPK cascades are composed of three cytoplasmic kinases in which the MAPKKK (MAP3K) phosphorylates and activates the MAPKK (MAP2K), which in turn phosphorylates and activates the MAPK. Once activated, MAPKs phosphorylate both cytoplasmic and nuclear substrates, controlling protein activity and regulating gene expression. There are six subfamilies of MAPKs: extracellular signal-regulated kinases (ERKs) 1 and 2, atypical ERK3/4, ERK5, atypical ERK7/8, Jun amino-terminal kinases (JNKs) 1, 2, and 3, and p38 kinase members p38α, β, γ, and δ. During embryonic development, JNK and p38 pathways are activated by mitogen-activated protein kinase kinase kinase 4 (MAP3K4) through activation of MAP2K4/7 and MAP2K3/6, respectively [13–15].

MAP3K4 and components of the MAP3K4 signaling cascade control gonadal sex determination [8–11]. Genetic deletion studies demonstrated that loss of MAP3K4 expression results in embryonic XY gonadal sex reversal due to reduced expression of *Sry* [8]. Importantly transgenic re-expression of MAP3K4 in *Map3k4*$^{-/-}$ mice rescues sex reversal [10]. Deletion of GADD45γ, an upstream activator of MAP3K4, causes male to female sex reversal in mouse embryos and adults [9]. p38 MAPK signaling is disrupted in both *Map3k4*$^{-/-}$ and *Gadd45*$\gamma^{-/-}$ embryonic gonads due to reduced phosphorylation of p38 and its target GATA4 [9]. Gonadal sex reversal is also observed in XY embryos with co-deletion of p38$\alpha^{-/-}$ and p38$\beta^{-/-}$ [9]. MAP2K3 and MAP2K6 phosphorylate and activate p38. Both MAP2K3 and MAP2K6 are activated by MAP3K4 in response to extracellular stimuli during development [15]. Mice with deletion of *Map2k3* or *Map2k6* do not show overt abnormalities in XY gonads in the C57BL/6 J background [11]. However, changes in sex determination are observed with deletion of *Map2k3* or *Map2k6* in the C57BL/6 J.Y^{AKR} background, which is highly sensitized to disruption of testis-determining genes due to harboring

the weaker *Sry* allele (Sry^{AKR}) [11, 16, 17]. Deletion of *Map2k3* in the C57BL/6 J.Y^{AKR} background causes ovotestis formation, and *Map2k6* deletion resulted in complete sex reversal [11].

Although deletion of MAP3K4 and several MAP3K4 signaling cascade components results in gonadal sex reversal, it is unknown if MAP3K4 kinase activity is required for sex determination [9]. MAP3K4 has many kinase-independent functions that do not require MAP3K4 catalytic activity [14, 18, 19]. For example, MAP3K4 interacts with many other proteins such as TRAF4, AXIN, and HDAC6 independent of MAP3K4 kinase activity [14, 18, 19]. In the MAP3K4 knockout model, loss of MAP3K4 protein results in the absence of interactions with these proteins that may also be associated with sex determination. To determine if the kinase activity of MAP3K4 is required for sex determination, we used a knock-in mouse model for MAP3K4 with inactivated MAP3K4 kinase activity through the targeted substitution of the active site lysine at position 1361 with an arginine in the endogenous *Map3k4* locus [15]. Mice with this mutation express full-length, kinase-inactive (KI) MAP3K4 protein, but KI MAP3K4 is unable to phosphorylate downstream targets MAP2K3/6 and MAP2K4/7 [15]. Importantly, KI MAP3K4 retains the ability to bind AXIN, TRAF4, and HDAC6 [14, 18, 19]. This approach allows us to maintain MAP3K4 protein–protein interactions while simultaneously examining the role of MAP3K4 kinase activity during sex determination. Here, we report that despite the high penetrance lethality of the homozygous inactivation of MAP3K4 kinase activity ($Map3k4^{KI/KI}$), we were able to examine the female to male sex ratio in surviving adults. We found that $Map3k4^{KI/KI}$ adults exhibited a 4:1 female-biased sex ratio, suggesting potential problems with sex determination. We discovered that many of $Map3k4^{KI/KI}$ adults with an external female phenotype were genetically XY. Importantly, $Map3k4^{KI/KI}$ XY adults with a female phenotype and gonadal sex reversal were infertile with several defects in reproductive organs. $Map3k4^{KI/KI}$ XY adults with a female phenotype were smaller in size and weight compared to either age matched female or male $Map3k4^{WT/WT}$ animals. Further, we show that E11.5 XY $Map3k4^{KI/KI}$ embryos failed to express *Sry*, consistent with disruption of male gonadal sex determination. Gonads from XY $Map3k4^{KI/KI}$ embryos at E13.5 and E14.5 displayed an ovarian morphology and dysregulated expression of markers for ovaries and testes. Together, our findings demonstrate the requirement of MAP3K4 kinase activity during male gonadal sex determination in mice.

Materials and methods

Mouse models and fertility trials

Kinase-inactive MAP3K4 mice having a point substitution of the active site lysine at position 1361 to arginine were generated as previously described [15]. These mice called $Map3k4^{KI}$ for kinase-inactive having a mixed 129SvEv/C57BL/6 N background were backcrossed one time with C57BL/6 N. All experimental samples isolated and all embryos and adults shown were performed in this genetic background. Due to the lethality of the mutation, mice were maintained through $Map3k4^{WT/KI}$ heterozygote crosses. Mice generated for mouse colony maintenance were genotyped for the KI mutation and for their genotypic sex.

For examination of fertility, timed matings were performed. Mice were checked each morning for fourteen days for a copulatory plug, and then were separated. $Map3k4^{WT/WT}$ female mice were mated with $Map3k4^{WT/WT}$ male mice. $Map3k4^{WT/KI}$ and $Map3k4^{KI/KI}$ phenotypically female mice were mated with heterozygote $Map3k4^{WT/KI}$ male mice. The fertility of all $Map3k4^{WT/WT}$ and $Map3k4^{WT/KI}$ males used in the fertility tests was demonstrated. The statistical power of these experiments was limited by the rare survival of $Map3k4^{KI/KI}$ adults. For examination of E11.5, E13.5, and E14.5 embryos, timed matings of male and female $Map3k4^{WT/KI}$ mice were performed. Noon on the day of the detected copulatory plug was considered E0.5. Pregnant females were humanely euthanized, and embryos were isolated, imaged, and euthanized by decapitation. Gonads were isolated as previously described and placed together in RNAlater [20].

The ethics statement

All experiments using animals were approved by the Institutional Animal Care and Use Committee (IACUC) at the University of Memphis. All experiments using animals were performed according to institutional and National Institutes of Health guidelines and regulations.

Map3k4^{KI} mutation genotyping

Genomic DNA was isolated from adult mouse tail snips using a salt and ethanol extraction method. Each 1 mm tail snip was digested overnight at 55 °C using 600 µL of TNES (50 mM Tris, 0.4 M NaCl, 100 mM EDTA, 0.5% SDS) and 0.58 mg/mL Proteinase K. On the next day, 167 µL of saturated NaCl was added and the solution was spun at 16 200 x g for 30 min at room temperature. The supernatant was transferred to a new tube, an equal volume of 100% ethanol was added, and centrifugation was performed at 16 200 x g for 30 min at 4 °C. The ethanol was decanted, the DNA pellet was washed with 500 µL of 70% ethanol, and spun at 16 200 x g for 5 min at 4 °C. Residual ethanol was removed, and the DNA was resuspended in water. The samples were placed in a heat block at 60 °C for 10 min to evaporate any residual ethanol. Genomic DNA was isolated from embryos according to the manufacturer instructions using the QIAamp DNA Micro Kit. Genotyping for the $Map3k4^{KI}$ mutation was performed using PCR and Platinum Taq DNA polymerase (Invitrogen). PCR conditions consisted of one cycle of initial denaturation for 3 min at 94 °C followed by 32 cycles at 94 °C for 20 s, 61 °C for 1 min, and 72 °C for 3 min with a final extension for 3 min at 72 °C. Primers designed to detect *Map3k4* and the neomycin insertion in $Map3k4^{KI}$ are listed in Supplementary Table S1. Amplified PCR products were resolved in a 1% agarose gel using ethidium bromide for detection and the Bio-Rad Chemidoc Touch for imaging.

Sex genotyping

Adult mice and embryos were chromosomally sexed using PCR and primers that amplify *Ube1y1* and *Ube1x* genes simultaneously (Supplementary Table S1) [21]. PCR conditions consisted of one cycle of initial denaturation for 3 min at 95 °C followed by 32 cycles at 95 °C for 20 s, 57 °C for 1 min, and 72 °C for 30 s with a final extension for 3 min at 72 °C using Platinum Taq DNA polymerase (Invitrogen). Amplified PCR products were resolved in a 2% agarose gel using ethidium bromide for detection and the Bio-Rad Chemidoc Touch for imaging.

Cell lysis and Western blotting

Whole-cell lysates from trophoblast stem cells were prepared as previously described [15, 22]. Briefly, whole cell lysates were harvested using buffer A (20 mM Tris pH 7.4, 150 mM NaCl, 1 mM EDTA, 1 mM EGTA and 1% Triton) with protease inhibitors (1 mM PMSF and 100 KIU/ml aprotinin) and phosphatase inhibitors (2 mM sodium vanadate and 20 mM sodium fluoride). Samples were

analyzed using SDS-PAGE and Western blotting. The following antibodies were used: mouse anti-MAP3K4 (Sigma #M7194, 1:3000, AB_477232), rabbit anti-Phospho-p38 (Cell Signaling #9211, 1:1000, AB_331641), rabbit anti-p38 (Cell Signaling #8690, 1:1000, AB_10999090), mouse anti-α-tubulin (Sigma #T9026, 1:5000, AB_477593), rabbit anti-Phospho-MKK3/6 (Cell Signaling #12280, 1:1000, AB_2797868), and rabbit anti-MKK3 (Cell Signaling #8535, 1:1000, AB_11220233).

Real-time quantitative PCR

Total cellular RNA was isolated at E11.5 and E13.5 from combined gonads per embryo using an RNeasy Plus Micro Kit (QIAGEN), and cDNA was prepared from total gonad RNA using the High-Capacity cDNA reverse transcription kit (ThermoFisher Scientific) as previously described [20, 23]. Gene expression was measured using iTaq Universal SYBR Green Supermix (Bio-Rad) and the Bio-Rad CFX96 Touch. Gene expression levels were calculated using $2^{-\Delta\Delta CT}$ method and normalized to the reference gene *Hprt1*. Primers used are specified in Supplementary Table S1.

Evaluation of reproductive tracts

Reproductive tracts were dissected, assessed for the absence or presence of a complete, intact reproductive tract, and imaged using a Leica stereomicroscope. Two of the XY *Map3k4*$^{KI/KI}$ adults had only one uterine horn and one ovary. The female reproductive tracts of the remaining XY *Map3k4*$^{KI/KI}$ adults were complete. Reproductive tracts were fixed in 10% formalin and processed for paraffin embedding and sectioning. Sections were stained with hematoxylin and eosin (H&E) and evaluated by a veterinary pathologist. Serial sections of both ovaries per animal were evaluated for size, morphology, and the presence of follicles.

Statistics and reproducibility

Statistical analyses were performed using Prism7 (version 7.0, GraphPad software). Prism7 was used to perform a two-tailed unpaired Student *t* test. $P < 0.05$ was considered statistically significant.

Results

Female-biased sex ratio in *Map3k4*$^{KI/KI}$ mice and embryonic lethality at E13.5

Components of the MAP3K4 signaling cascade have previously been shown to be required during sex determination [8–11]. MAP3K4 has both kinase-dependent and kinase-independent functions, and it is unknown if the kinase activity of MAP3K4 is essential for sex determination. To define the role of MAP3K4 kinase activity during sex determination, we used KI MAP3K4 mice having a point substitution of the active site lysine at position 1361 to arginine [15]. Cells isolated from *Map3k4*$^{KI/KI}$ embryos expressed full-length kinase-inactive MAP3K4 that failed to phosphorylate downstream targets MAP2K3 and MAP2K6 resulting in loss of phosphorylation of p38 (Figure 1A). Mice generated from *Map3k4*$^{WT/KI}$ heterozygote crosses were genotyped for the KI mutation. A non-Mendelian ratio of mouse adults homozygous for *Map3k4*$^{KI/KI}$ was observed with only 4.5% of the adult mice being homozygous for *Map3k4*$^{KI/KI}$, suggesting potential embryonic lethality with MAP3K4 kinase inactivation (Table 1). Examination of embryos isolated at E13.5 from timed matings of male and female heterozygote *Map3k4*$^{WT/KI}$ mice showed that only 13.5% of embryos were homozygous for *Map3k4*$^{KI/KI}$ (Table 2). This number represents half of the expected Mendelian ratio for *Map3k4*$^{KI/KI}$ embryos (Table 2). Of these *Map3k4*$^{KI/KI}$ embryos, 71.4% exhibited neural tube defects including spina bifida and exencephaly (Table 2). The high percentage of embryonic resorptions detected at E13.5 was consistent with the loss of half of the *Map3k4*$^{KI/KI}$ embryos at earlier stages of development (Table 2). Together, these data suggest that loss of *Map3k4*$^{KI/KI}$ embryos and mice at multiple stages of development is due to MAP3K4 kinase inactivation. In addition to these developmental defects, examination of surviving adult *Map3k4*$^{KI/KI}$ mice showed a 4:1 female-biased sex ratio, suggesting that MAP3K4 kinase activity may play an important role during sex determination (Table 1).

Loss of MAP3K4 kinase activity causes a sex reversal phenotype in XY *Map3k4*$^{KI/KI}$ mice

The chromosomal sex of phenotypically male and female *Map3k4*$^{KI/KI}$ mice was examined (Supplementary Figure S1A). We found that many of the *Map3k4*$^{KI/KI}$ phenotypic females were positive for the Y chromosome. Importantly, these adult XY *Map3k4*$^{KI/KI}$ individuals showed external genitalia comparable to *Map3k4*$^{WT/WT}$ female controls (Figure 1B). Average anogenital distance (AGD) of XY *Map3k4*$^{KI/KI}$ mice with sex reversal was significantly different than XY *Map3k4*$^{WT/WT}$ phenotypic males (Figure 1C). Importantly, the AGD of XY *Map3k4*$^{KI/KI}$ mice with sex reversal was not significantly different from XX *Map3k4*$^{WT/WT}$ and *Map3k4*$^{KI/KI}$ females (Figure 1C). These data demonstrate that loss of MAP3K4 kinase activity resulted in sex reversal in the majority of XY mice homozygous for MAP3K4 inactivation.

Reduced size and weight of XY *Map3k4*$^{KI/KI}$ mice with sex reversal

Examination of XY *Map3k4*$^{KI/KI}$ mice with a female phenotype revealed significant differences in body size. As expected, XY *Map3k4*$^{KI/KI}$ mice with a female phenotype were smaller than XY *Map3k4*$^{WT/WT}$ males (Figure 2A–C). Figure 2A–C shows the body size of three different XY *Map3k4*$^{KI/KI}$ mice with a female phenotype relative to *Map3k4*$^{WT/WT}$ females and males. Comparison of average weight showed significant decreases in the weight of XY *Map3k4*$^{KI/KI}$ mice with a female phenotype relative to XY *Map3k4*$^{WT/WT}$ males measured at either 4 or 6 months (Figure 2D and E). Surprisingly, the average weight of the XY *Map3k4*$^{KI/KI}$ adult mice with sex reversal was also significantly less than the average weight of XX *Map3k4*$^{WT/WT}$ females measured at either 4 or 6 months (Figure 2D and E). In addition, XY *Map3k4*$^{KI/KI}$ adult mice with sex reversal weighed less than XX *Map3k4*$^{KI/KI}$ females measured at 6 months (Figure 2E). In contrast, there were no statistically significant differences in the weights of XX *Map3k4*$^{WT/WT}$ and XX *Map3k4*$^{KI/KI}$ females (Figure 2E and Supplementary Figure S1B). These data suggest that loss of MAP3K4 kinase activity in XY *Map3k4*$^{KI/KI}$ mice with a sex reversal phenotype disrupts both growth and weight.

Characterization of reproductive capacity and gonadal phenotype in adult XY *Map3k4*$^{KI/KI}$ mice with sex reversal

Next, we examined the impact of loss of MAP3K4 kinase activity on the reproductive capacity of both XX and XY *Map3k4*$^{KI/KI}$ phenotypic females. Timed matings of XX or XY *Map3k4*$^{KI/KI}$ phenotypic female mice with *Map3k4*$^{WT/KI}$ males were performed. Mice were assessed daily for 14 days for the presence of a copulatory plug. Then, mice were separated and examined daily for signs of

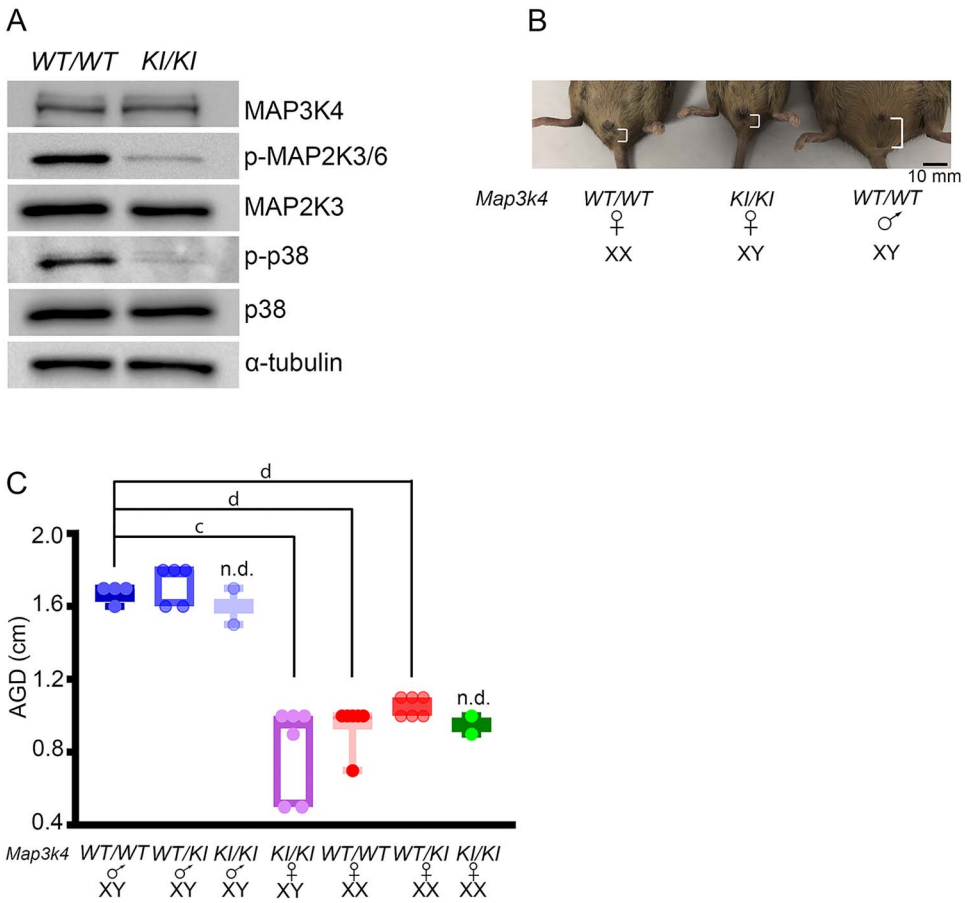

Figure 1. Sex reversal phenotype in XY *Map3k4*$^{KI/KI}$ adult mice. (A) Cells isolated from *Map3k4*$^{KI/KI}$ embryos express full-length kinase-inactive MAP3K4 but have reduced phosphorylation (p) of MAP2K3/6 and p38 MAPK. Western blots are representative images from three biologically independent experiments. (B) Phenotypic comparison of external genitalia of adult mice. Anogenital distance (AGD) of representative XY *Map3k4*$^{KI/KI}$ mouse with sex reversal is comparable to XX *Map3k4*$^{WT/WT}$ female. AGD is indicated using square brackets. (C) Average AGD was quantified in *Map3k4*$^{WT/WT}$, *Map3k4*$^{WT/KI}$, and *Map3k4*$^{KI/KI}$ male and female mice. Data are displayed as box plots and each individual is plotted as one dot. (B-C) *Map3k4* genotype, sex phenotype, and sex genotype are indicated below each panel. Statistical analyses were performed relative to XY *Map3k4*$^{WT/WT}$ mice where the lowercase letters indicates statistically significant differences: c, $P < 0.001$; d, $P < 0.0001$; Student *t* test; n.d., not determined due to only two individuals; XY *Map3k4*$^{WT/KI}$ mice were not significantly different from XY *Map3k4*$^{WT/WT}$ mice.

Table 1. Female-biased sex ratios in adult mice deficient in MAP3K4 kinase activity.

Map3k4 Genotype	Male	Female	Total
WT/WT	40 (16.3%)	31 (12.6%)	71 (28.86%)
WT/KI	76 (30.9%)	88 (35.8%)	164 (66.66%)
KI/KI	2 (0.8%)	9 (3.7%)	11 (4.5%)
Total	118 (48.0%)	128 (52.0%)	246 (100%)

Table 2. Reduced numbers of *Map3k4*$^{KI/KI}$ kinase-inactive embryos at E13.5 indicating embryonic lethality.

Map3k4 Genotype	% of total embryos	% with neural tube defects	*n* of embryos
WT/WT	28.8	0	15
WT/KI	44.2	0	23
KI/KI	13.5	71.4	7
Resorption	13.5	0	7
Total	100	NA	52

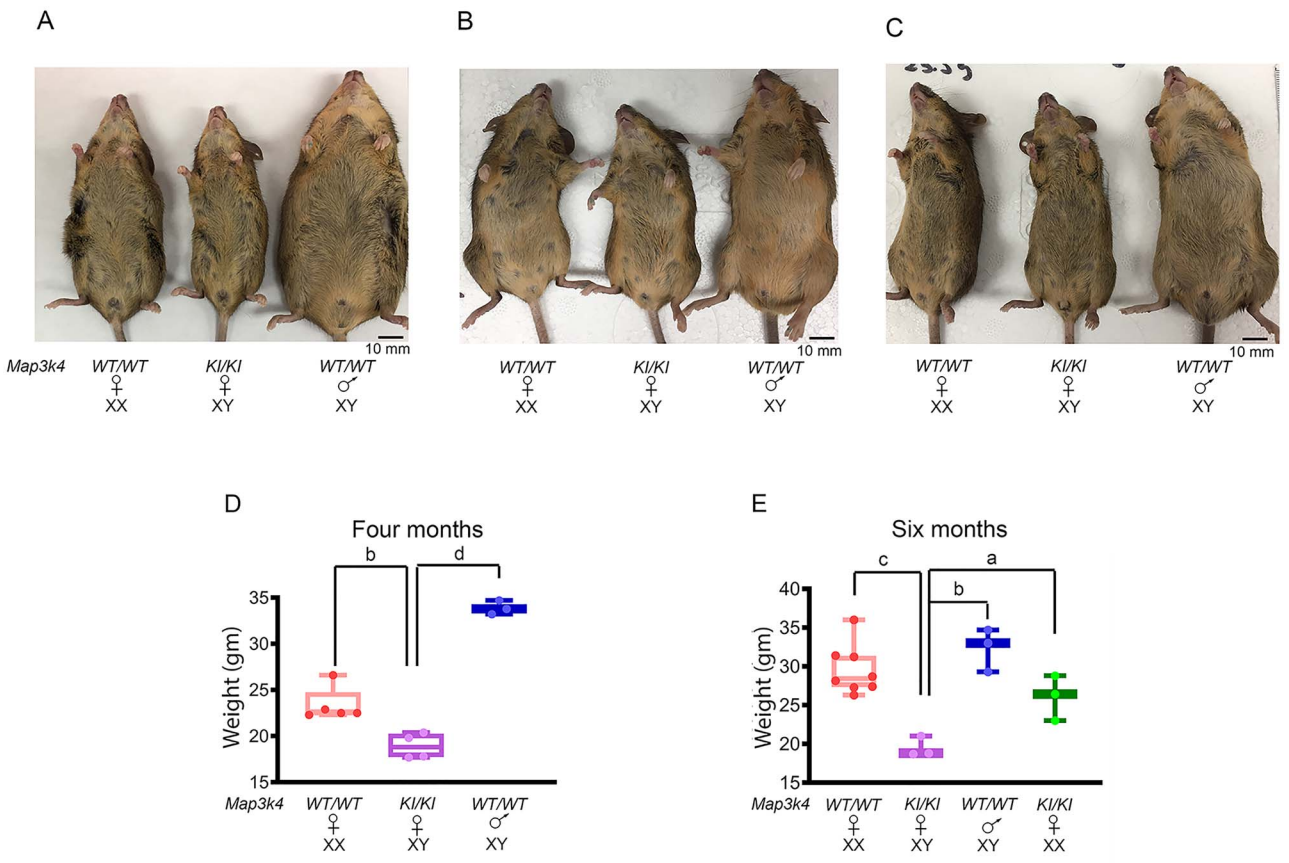

Figure 2. Reduced body size and weight in XY *Map3k4*$^{KI/KI}$ adult mice having a gonadal sex reversal phenotype. (A-C) Body size of three individual representative XY *Map3k4*$^{KI/KI}$ mice with sex reversal compared to *Map3k4*$^{WT/WT}$ female and male mice. (A) Aged 6 months. (B-C) Aged 5 months. (D, E) Reduced average body weight of XY *Map3k4*$^{KI/KI}$ adult mice with sex reversal compared to phenotypic male and female *Map3k4*$^{WT/WT}$ mice at 4 months (D) or 6 months (E). (D, E) Data are displayed as box plots, and each dot represents one individual. The lowercase letters indicate statistically significant differences: a, $P < 0.05$; b, $P < 0.01$; c, $P < 0.001$; d, $P < 0.0001$; Student *t* test.

pregnancy and the birth of pups. These results were compared to timed matings of *Map3k4*$^{WT/WT}$ females with *Map3k4*$^{WT/WT}$ males and timed matings of *Map3k4*$^{WT/KI}$ females with *Map3k4*$^{WT/KI}$ males. Importantly, the fertility of *Map3k4*$^{WT/WT}$ and *Map3k4*$^{WT/KI}$ males used in these experiments was validated. With the exception of one female, all *Map3k4*$^{WT/WT}$ females had a copulatory plug within the first 7 days of pairing (Supplementary Table S2). All *Map3k4*$^{WT/WT}$ females were pregnant and had offspring, regardless of the detection of the plug (Supplementary Table S2). XX *Map3k4*$^{WT/KI}$ and XX *Map3k4*$^{KI/KI}$ females required more days to plug. Out of nine mated XX *Map3k4*$^{WT/KI}$ females, seven individuals had copulatory plugs, and only six of them gave offspring. Only one of the two examined XX *Map3k4*$^{KI/KI}$ female mice had offspring, and all the offspring died at birth due to severe developmental defects, including exencephaly and spina bifida. These data suggest that heterozygous and homozygous loss of MAP3K4 kinase activity in XX individuals resulted in reduced reproductive capacity. Importantly, sex-reversed XY *Map3k4*$^{KI/KI}$ mice were able to mate and had copulatory plugs in 60% of the examined animals, indicating female mating behavior. However, they were infertile, showing no signs of pregnancy and yielding no offspring (Supplementary Table S2). Although these data are consistent with reduced fertility of XX *Map3k4*$^{KI/KI}$ mice and XY *Map3k4*$^{KI/KI}$ mice with sex reversal, the limited numbers of viable *Map3k4*$^{KI/KI}$ mice were too low to definitively demonstrate reduced fertility.

To further assess the reproductive status of kinase-inactive MAP3K4 mice, necropsies were performed. During this 24-month study, only two adult phenotypically male XY *Map3k4*$^{KI/KI}$ mice were obtained. Unlike littermate *Map3k4*$^{WT/WT}$ males that showed overtly normal reproductive tracts, both XY *Map3k4*$^{KI/KI}$ phenotypic male mice displayed cryptorchidism (Supplementary Figure S2A–C). Testis size was reduced in XY *Map3k4*$^{KI/KI}$ mice relative to *Map3k4*$^{WT/WT}$ littermates (Supplementary Figure S2D). Due to the rare survival of XY *Map3k4*$^{KI/KI}$ phenotypic male adults, we were unable to determine the frequency of this phenotype or the statistical significance of the changes in body size or weight (Supplementary Figure S2E).

Necropsies were also performed on phenotypically female mice. Figure 3 shows macroscopic images and histological sections from four different XY *Map3k4*$^{KI/KI}$ mice individuals with sex reversal compared to two XX *Map3k4*$^{WT/WT}$ females. All XX *Map3k4*$^{WT/WT}$ females displayed normal reproductive tracts with identifiable ovaries and uterine structures (Figure 3A). H&E staining of ovarian sections from XX *Map3k4*$^{WT/WT}$ females showed numerous corpus lutea and examples of follicles at all stages of development (Figure 3B). Similar to *Map3k4*$^{WT/WT}$, all three XX *Map3k4*$^{KI/KI}$

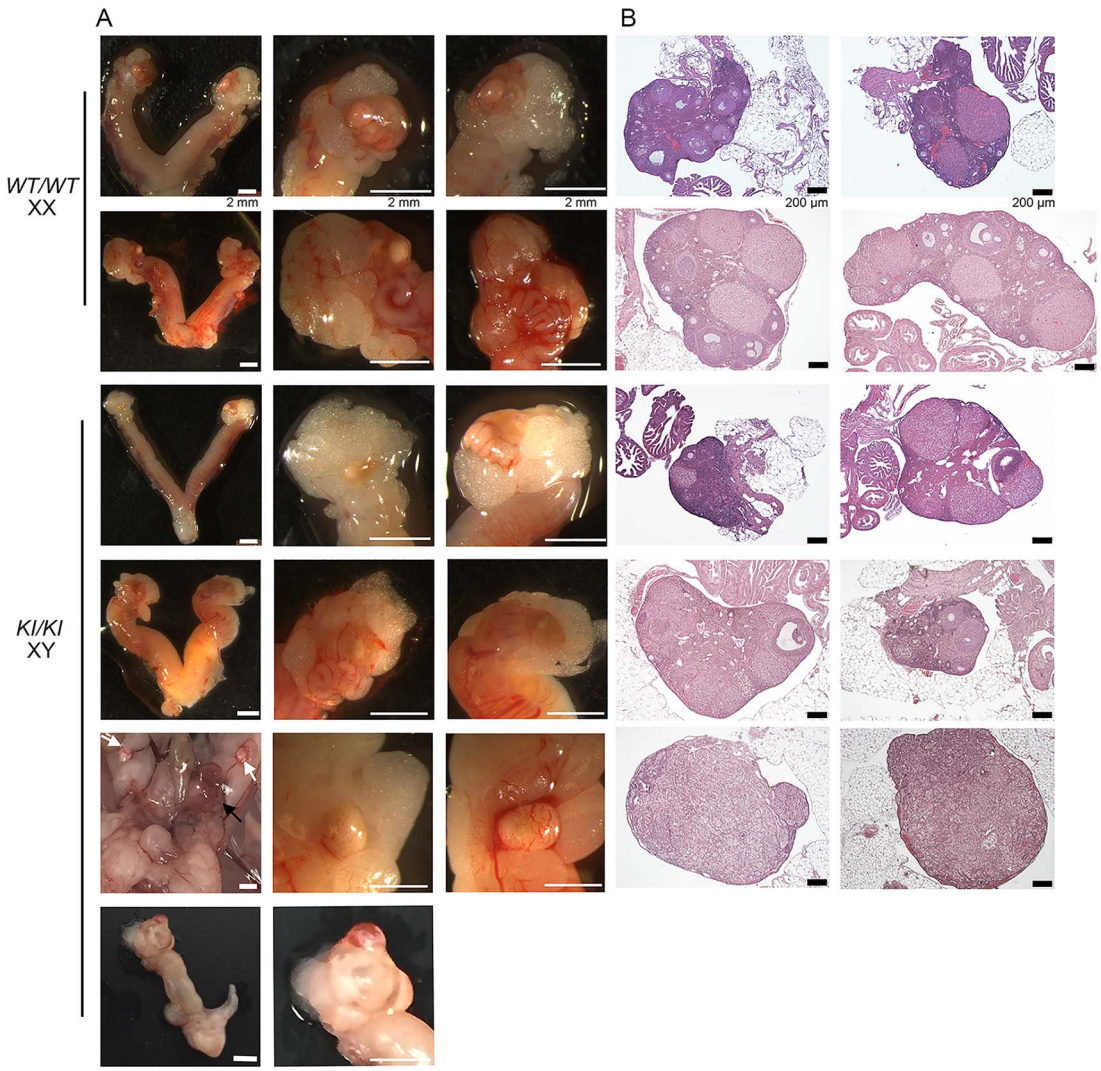

Figure 3. Gonadal sex reversal phenotype in XY *Map3k4*$^{KI/KI}$ adult mice. (A) Representative macroscopic images of adult reproductive tracts and enlarged images of ovaries from adult XX *Map3k4*$^{WT/WT}$ and XY *Map3k4*$^{KI/KI}$ mice. White arrows indicate location of primitive gonads. Black arrow indicates position of uterine structure. (B) Histological examination of H&E stained paraffin sections of XX *Map3k4*$^{WT/WT}$ and XY *Map3k4*$^{KI/KI}$ adult ovaries.

female mice displayed overtly normal reproductive tracts, and ovaries showed all stages of follicle development (data not shown). Uterine and ovarian morphology was extremely variable among the XY *Map3k4*$^{KI/KI}$ mice with sex reversal. Figure 3 shows four examples of different phenotypes observed. Two XY *Map3k4*$^{KI/KI}$ mice were missing one ovary and one uterine horn, suggesting disruption of reproductive tract development (Figure 3 and data not shown). One XY *Map3k4*$^{KI/KI}$ mouse had very primitive gonads, completely lacking any evidence of follicle development (Figure 3). Although there were differences in ovarian size, the remaining XY *Map3k4*$^{KI/KI}$ mice displayed evidence of corpus lutea and follicles at many stages of development (Figure 3B). Together, these data suggest that XY *Map3k4*$^{KI/KI}$ mice with gonadal sex reversal are infertile, and infertility is due in part to reproductive tract defects.

Gonadal sex reversal phenotype in embryos homozygous for MAP3K4 kinase inactivation

The impact of MAP3K4 kinase inactivation on gonadal sex determination in developing bipotential gonads was examined using embryos isolated from timed matings of male and female heterozygote *Map3k4*$^{WT/KI}$ mice. Embryos were examined for *Map3k4* and sex genotypes. First, we examined the gonadal sex determining stage of E11.5. Unlike E13.5 that showed a 50% reduction in *Map3k4*$^{KI/KI}$ embryos, *Map3k4*$^{KI/KI}$ embryos were present at Mendelian ratios at E11.5 (Tables 2 and 3). However, three of the eight XY *Map3k4*$^{KI/KI}$ embryos isolated at E11.5 were developmentally delayed, lacking hindlimb buds (data not shown). Although the majority of XY *Map3k4*$^{KI/KI}$ embryos isolated at E11.5 were at developmental stages similar to *Map3k4*$^{WT/WT}$ littermates, many showed neural tube defects, including exencephaly and open posterior neuropore (Figure 4A–E). *Sry* transcript expression was measured at E11.5 in embryos that were not developmentally delayed. Loss of *Sry* expression was observed in all five XY *Map3k4*$^{KI/KI}$ embryos (Figure 4F). These data suggested that MAP3K4 kinase activity is required for *Sry* expression.

SRY promotes the expression of Sertoli cell markers like *Sox9* and *Dhh*. The expression of *Sox9* and *Dhh* are required for driving testis development in XY individuals and antagonizing the ovary-determining pathways [8, 24, 25]. Gonads were dissected from

Table 3. *Map3k4* and sex chromosome genotyping of embryos isolated at E11.5 from *Map3k4*$^{WT/KI}$ heterozygote crosses.

Map3k4 Genotype	Male XY	Female XX	Total
WT/WT	4 (9.8%)	6 (14.6%)	10 (24.4%)
WT/KI	13 (31.7%)	7 (17.1%)	20 (48.8%)
KI/KI	8 (19.5%)	3 (7.3%)	11 (26.8%)
Total	25 (61%)	16 (39%)	41 (100%)

Six resorptions were detected.

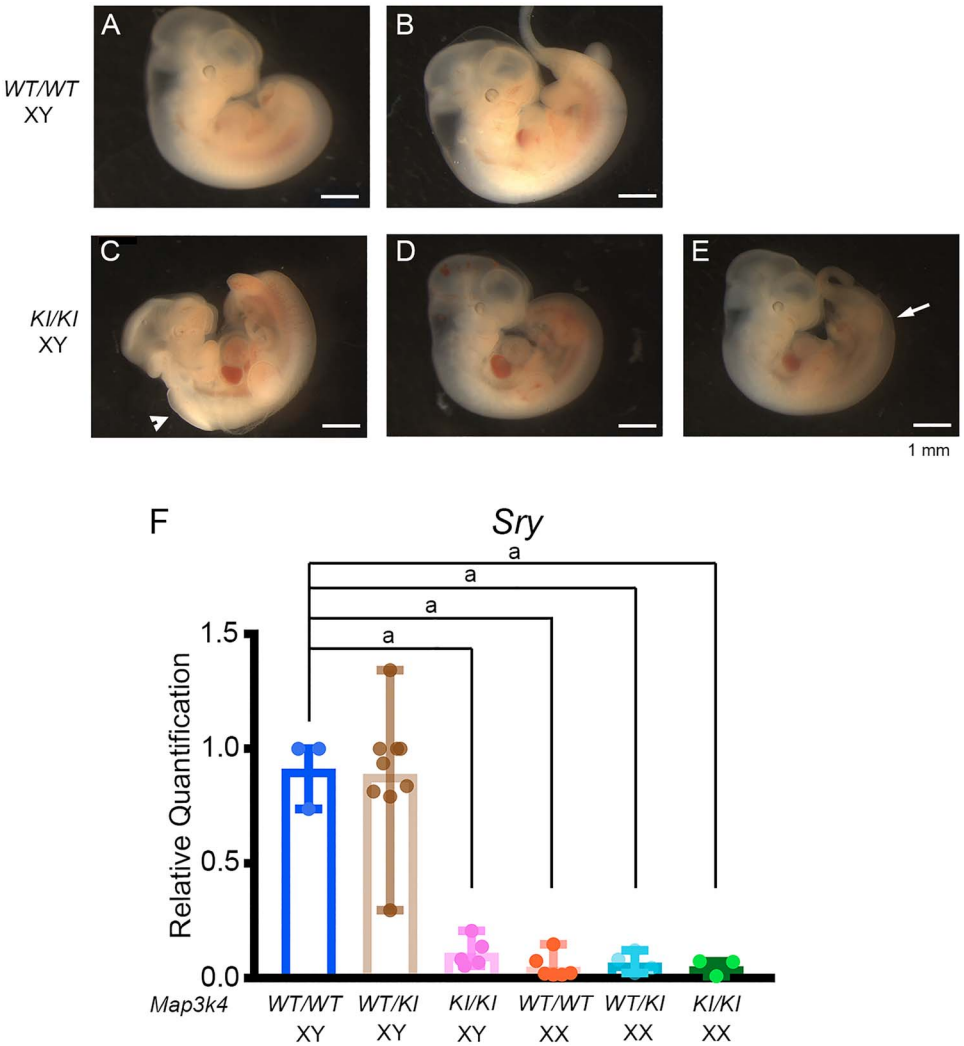

Figure 4. *Sry* expression is absent in most XY *Map3k4*$^{KI/KI}$ embryos at E11.5. (A-E) Representative images of E11.5 embryos generated from crosses of *Map3k4*$^{WT/KI}$ mice. White arrowhead indicates exencephaly, and white arrow indicates open posterior neuropore. (F) Relative *Sry* expression in E11.5 embryos generated from crosses of *Map3k4*$^{WT/KI}$ mice. Transcript expression in E11.5 gonads measured by qPCR was normalized to *Hprt1*. Data are expressed as a fold change relative to XY *Map3k4*$^{WT/WT}$. Data shown are the mean ± SEM, and each point represents one embryo. Statistical analyses were performed relative to XY *Map3k4*$^{WT/WT}$ embryos where the lowercase letter a indicates $P < 0.05$; Student *t* test; XY *Map3k4*$^{WT/KI}$ embryos were not significantly different from XY *Map3k4*$^{WT/WT}$ embryos.

XY and XX *Map3k4*$^{WT/WT}$ and *Map3k4*$^{KI/KI}$ E13.5 embryos and examined for the transcript expression of Sertoli cell markers (*Sox9* and *Dhh*), ovarian marker (*Irx3*) and the meiosis marker (*Stra8*) using qPCR. *Sox9* and *Dhh* transcripts were expressed at higher levels in control XY *Map3k4*$^{WT/WT}$ E13.5 embryonic gonads relative to XX *Map3k4*$^{WT/WT}$ and XX *Map3k4*$^{KI/KI}$ gonads (Figure 5A). XY *Map3k4*$^{KI/KI}$ gonads showed a 44% and 95% decrease in expression of *Sox9* and *Dhh*, respectively, compared to XY *Map3k4*$^{WT/WT}$ gonads (Figure 5A). *Irx3* and *Stra8* are expressed during ovarian development [26, 27]. XX *Map3k4*$^{WT/WT}$ and XX *Map3k4*$^{KI/KI}$ E13.5 ovaries expressed higher transcript levels of *Irx3* and *Stra8* compared to XY *Map3k4*$^{WT/WT}$ E13.5 gonads (Figure 5A). In contrast, E13.5 XY *Map3k4*$^{KI/KI}$ gonads showed a 2.9-fold increase in *Irx3* compared to XY *Map3k4*$^{WT/WT}$ gonads (Figure 5A). The statistical power of these experiments was severely limited due to the difficulty in obtaining viable *Map3k4*$^{KI/KI}$ embryos at E13.5. Seven of the

52 conceptuses from six litters examined were resorptions, having severely decayed embryos that could not be genotyped (Table 2). Of the seven viable *Map3k4*$^{KI/KI}$ embryos, two were extremely developmentally delayed, and we were unable to isolate their gonads. One XY *Map3k4*$^{KI/KI}$ embryo had only one gonad, and was not analyzed further. These data suggest that inactivation of MAP3K4 kinase activity results in loss of molecular pathways driving testis development.

The impact of MAP3K4 kinase activity was examined on gonadal morphology in embryos isolated at E14.5. Although three litters were examined, only one litter had XY *Map3k4*$^{KI/KI}$ embryos. Gonads from control littermate XY *Map3k4*$^{WT/KI}$ embryos showed the presence of testis cords, and gonads from XX *Map3k4*$^{WT/KI}$ embryos showed normal ovarian morphology (Figure 5B). XX *Map3k4*$^{KI/KI}$ gonads were similar to XX *Map3k4*$^{WT/WT}$ controls (data not shown). Of the three obtained XY *Map3k4*$^{KI/KI}$ embryos, all gonads lacked testis cords and displayed an overt ovarian morphology (Figure 5B). These effects on gonadal morphology were consistent with the loss of *Sry* expression at E11.5 and the loss of *Sox9* expression at E13.5 in gonads from XY *Map3k4*$^{KI/KI}$ embryos. Together, these data support the critical role of MAP3K4 kinase activity in male gonadal sex determination pathways during gonadal development.

Discussion

MAP3K4 has both kinase-dependent and kinase-independent functions. Although the absence of MAP3K4 protein has been shown to result in gonadal sex reversal, these studies were unable to formally exclude the possibility that it may result from the loss of MAP3K4 kinase-independent functions [8, 9]. Further, it has been difficult to study the impact of the absence of MAP3K4 in adult animals, due to the lethality resulting from loss of MAP3K4 protein [8, 9, 15]. Here, we demonstrate the critical role of the kinase activity of MAP3K4 during gonadal sex determination. XY *Map3k4*$^{KI/KI}$ embryos expressing full-length kinase-inactive MAP3K4 lack expression of the testis determining gene, *Sry*. In addition, XY *Map3k4*$^{KI/KI}$ embryos have reduced expression of SRY regulated genes like *Sox9* and increased expression of ovarian markers, indicating gonadal sex reversal. Examination of gonadal morphology at E14.5 showed the lack of testis cords in XY *Map3k4*$^{KI/KI}$ gonads. Due to the survival of approximately 18% of the *Map3k4*$^{KI/KI}$ embryos to adulthood, we were able to examine adult *Map3k4*$^{KI/KI}$ mice, finding the majority of XY *Map3k4*$^{KI/KI}$ adult mice display a female phenotype based on external genitalia. Although these XY adult *Map3k4*$^{KI/KI}$ mice with gonadal sex reversal display female mating behavior, they are infertile. Necropsies of *Map3k4*$^{KI/KI}$ mice with sex reversal reveal the presence of female reproductive tracts. However, these tracts showed defects, including the partial absence of some components and the presence of very primitive gonads. Together, our work defines the requirement of MAP3K4 kinase activity during gonadal sex determination.

MAP3K4 is a large 180 kDa protein with a single catalytic domain and multiple interaction domains that have been shown to bind RAC, CDC42, TRAF4, CIN85, CCD1, AXIN, GSK3β, HDAC6, and GADD45α, $-\beta$, and $-\gamma$ [13, 14, 18, 19, 28–31]. Therefore, it was unknown if the sex reversal phenotype observed with the loss of MAP3K4 protein is due to loss of MAP3K4 kinase-dependent or independent function in *Map3k4* knockout mice. Using mice expressing full-length, kinase-inactive MAP3K4 from the endogenous *Map3k4* locus, we show the requirement of kinase activity of MAP3K4 during male gonadal sex determination [15]. KI MAP3K4 retains the ability to interact with almost all of its binding partners [14, 18, 19]. It has been difficult to examine the impact of MAP3K4 inactivation in adults due to the poor survival of mice homozygous for MAP3K4 inactivation (*Map3k4*$^{KI/KI}$) [15]. In an attempt to overcome this problem, heterozygous *Map3k4*$^{WT/KI}$ mice were backcrossed one time with C57BL/6 N mice creating a mixed 129SvEv/C57BL/6 N background. Similar to *Map3k4* knockout embryos, loss of MAP3K4 activity was sufficient to result in a sex reversal phenotype in the majority of *Map3k4*$^{KI/KI}$ XY embryos on the mixed 129SvEv/C57BL/6 N background. Although, the survival rate of adult *Map3k4*$^{KI/KI}$ mice remained poor, we were able to examine surviving adults for a sex reversal phenotype. Although the majority of *Map3k4*$^{KI/KI}$ XY embryos and adult mice examined in this study showed gonadal sex reversal, two surviving *Map3k4*$^{KI/KI}$ XY adult mice with a male phenotype were obtained. It is likely that this incomplete penetrance is due to the mixed genetic background that includes the 129SvEv background. The C57BL/6 J background is permissive to disruption of testis determination due in part to delayed expression of testis-determining genes and increased expression of ovary-determining genes [32–34]. However, we did not observe any sex reversal in XY *Map3k4*$^{WT/WT}$ controls. We also did not observe any sex reversal in adult *Map3k4*$^{KI/KI}$ XY mice on the 129SvEv background (data not shown). Similar to the C57BL/6 N, there is very low frequency of survival of *Map3k4*$^{KI/KI}$ adult mice on the 129SvEv background [22]. As expected, the sex reversal phenotype was maintained during backcrossing of mixed 129SvEv/C57BL/6 N background for five generations onto the C57BL/6 N background. However, no adult *Map3k4*$^{KI/KI}$ XY mice displaying a male phenotype were obtained from heterozygote mating of any of these backcrosses. Interestingly, *Map3k4*$^{KI/KI}$ XY adult mice with sex reversal displayed reduced size and average weight in comparison to XY and XX *Map3k4*$^{WT/WT}$ and XX *Map3k4*$^{KI/KI}$ littermates. The impact of loss of MAP3K4 kinase activity on adult mice has not previously been examined.

Previous studies have established the critical role of MAP3K4 and MAP3K4 signaling cascade components in gonadal sex determination. In seminal studies using an N-ethyl-N-nitrosurea (ENU) mutagenesis screen, Bogani et al. discovered a recessive mutation in *Map3k4* that they called boygirl (*byg*) [8]. The *Map3k4*^{byg} mutation created a premature stop codon, resulting in a predicted 382 amino acid fragment of the 1597 amino acid full-length MAP3K4 protein that lacks the kinase domain [8]. The protein stability and expression of this fragment is unknown [8]. Embryos with the *Map3k4*^{byg} mutation display embryonic gonadal sex reversal in XY individuals in a C57BL/6 J background demonstrating the essential role of MAP3K4 during male sex determination [8]. T-associated sex reversal (*Tas*) mice have a large deletion in chromosome 17 that includes the *Map3k4* locus [35–37]. *Tas* mice also display gonadal sex reversal [35–37]. Importantly, transgenic re-expression of MAP3K4 in either the *Map3k4* knockout or the *Tas* mice prevented gonadal sex reversal [10]. Several studies have dissected the individual roles of MAP3K4 signaling cascade components during sex determination. Knockout of GADD45γ, an upstream regulator of MAP3K4, results in formation of ovaries in XY embryos and adults [9]. Deletion of MAP3K4 direct downstream targets, MAP2K3 and MAP2K6, disrupts testis determination, but only in gonads of XY embryos on a sensitized C57BL/6 J Y^{AKR} background [11]. XY embryos homozygous for co-deletion of p38α and p38β exhibit complete gonadal sex reversal due to disruption of the p38 dependent testis-determining pathway GATA4-SRY-SOX9 [4, 9]. These studies defining the role

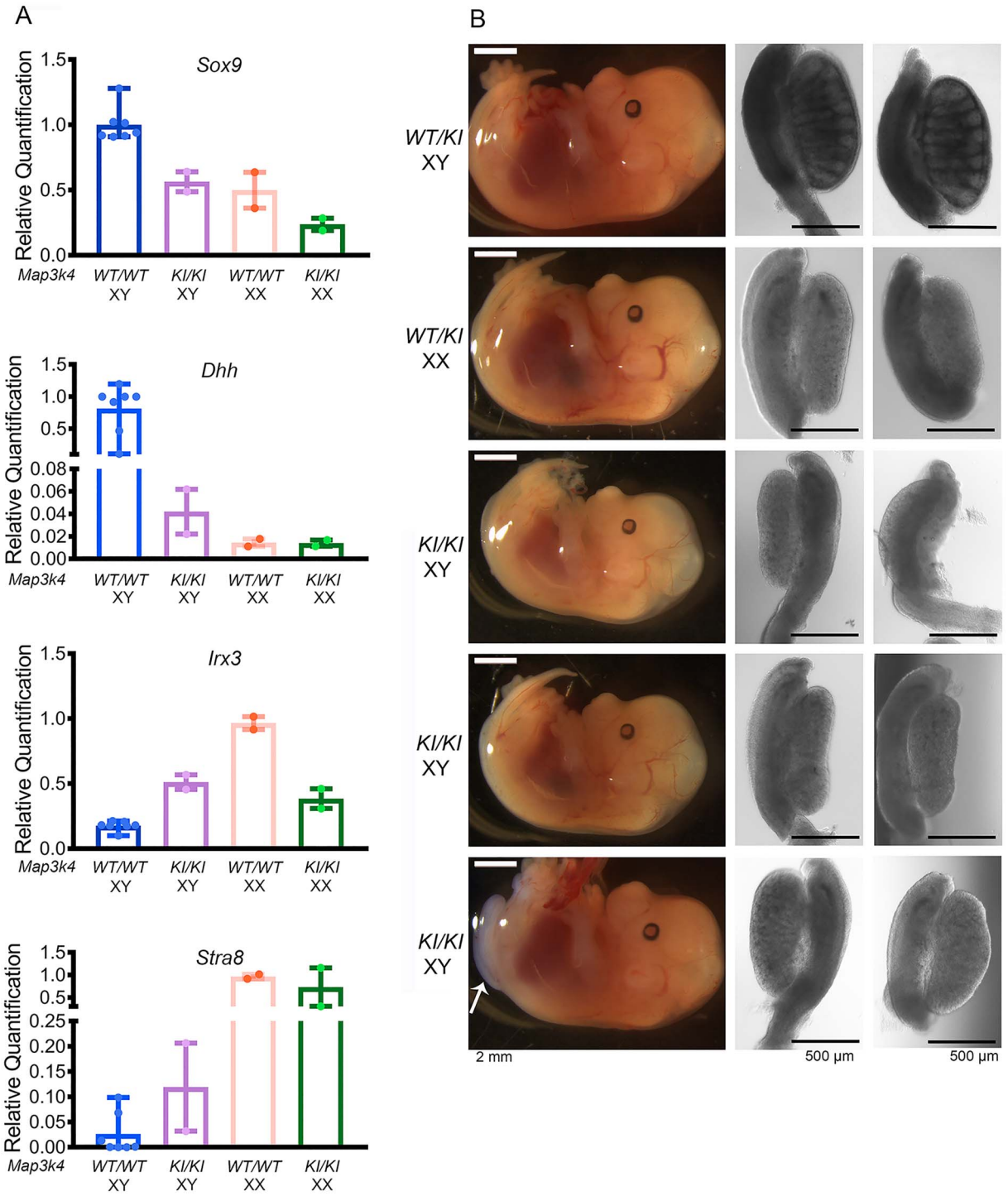

Figure 5. XY *Map3k4*$^{KI/KI}$ embryos display a gonadal sex reversal phenotype at E13.5 and E14.5. (A) Transcript expression of indicated genes in E13.5 gonads measured by qPCR was normalized to *Hprt1*. Data are expressed as a fold change relative to XY *Map3k4*$^{WT/WT}$ (*Sox9*, *Dhh*) or to XX *Map3k4*$^{WT/WT}$ (*Irx3*, *Stra8*). Data shown are the mean ± range, and each point represents one embryo. (B) Representative images of E14.5 embryos and gonads generated from crosses of *Map3k4*$^{WT/KI}$ mice. White arrow indicates spina bifida.

of MAP3K4 and its signaling components in sex determination are consistent with our findings demonstrating the kinase-activity dependence of MAP3K4 in the regulation of sex determination.

Our work provides very strong evidence that the kinase activity of MAP3K4 is required during testis determination. Our findings are consistent with several previous studies that have defined the critical roles of components of the MAP3K4 signaling cascade in gonadal sex determination. These studies demonstrate that the GADD45γ-MAP3K4-MAP2K3/6-p38 signaling cascade controls the expression of testis-determining genes. However, it remains unclear how this

signaling cascade controls the expression of *Sry* [9]. p38 dependent phosphorylation of GATA4 has been proposed, but the possibility of key roles for other transcription factors and chromatin modifiers remains [9]. A recent study has shown key roles for the epigenetic regulation of sex determination by the histone acetyltransferases p300 and CBP through the histone acetylation of the *Sry* promoter [38]. Our studies in trophoblast stem (TS) cells have shown that MAP3K4 promotes the JNK and p38 dependent phosphorylation and activation of p300 and CBP [39]. TS cells lacking MAP3K4 kinase activity have reduced CBP mediated acetylation of many genes leading to reduced expression, suggesting a possible molecular pathway for MAP3K4 regulation of sex determination [23, 39, 40]. Future studies will work to connect these pathways for the molecular control of mammalian gonadal sex determination.

Supplementary material

Supplementary material is available at *BIOLRE* online.

Acknowledgements

We thank Dr Omar Skalli and Ms. Lauren Thompson from the Integrated Microscopy Center at the University of Memphis for the processing and staining of reproductive tract samples for histology.

Conflict of interest: The authors declare that they have no conflicts of interest.

Author contributions

N.A.M.S., A.L.B., K.S., and A.N.A. performed experiments. N.A.M.S and A.N.A. designed experiments. R.R. performed necropsies and histological examination of animals. N.A.M.S., A.L.B., and A.N.A wrote and edited the manuscript.

Data availability

The authors declare that all data underlying this work are present in the published paper.

References

1. Warr N, Greenfield A. The molecular and cellular basis of gonadal sex reversal in mice and humans. *Wiley Interdiscip Rev Dev Biol* 2012; **1**:559–577.
2. Carre GA, Greenfield A. Characterising novel pathways in testis determination using mouse genetics. *Sexual Dev* 2014; **8**:199–207.
3. Stevant I, Nef S. Genetic control of gonadal sex determination and development. *Trends Genet* 2019; **35**:346–358.
4. Tanaka SS, Nishinakamura R. Regulation of male sex determination: genital ridge formation and Sry activation in mice. *Cell Mol Life Sci* 2014; **71**:4781–4802.
5. Karl J, Capel B. Sertoli cells of the mouse testis originate from the coelomic epithelium. *Dev Biol* 1998; **203**:323–333.
6. Schmahl J, Eicher EM, Washburn LL, Capel B. Sry induces cell proliferation in the mouse gonad. *Development* 2000; **127**:65–73.
7. Koopman P, Gubbay J, Vivian N, Goodfellow P, Lovell-Badge R. Male development of chromosomally female mice transgenic for Sry. *Nature* 1991; **351**:117–121.
8. Bogani D, Siggers P, Brixey R, Warr N, Beddow S, Edwards J, Williams D, Wilhelm D, Koopman P, Flavell RA, Chi H, Ostrer H et al. Loss of mitogen-activated protein kinase kinase kinase 4 (MAP3K4) reveals a requirement for MAPK signalling in mouse sex determination. *PLoS Biol* 2009; **7**:e1000196.
9. Warr N, Carre GA, Siggers P, Faleato JV, Brixey R, Pope M, Bogani D, Childers M, Wells S, Scudamore CL, Tedesco M, del Barco Barrantes I et al. Gadd45gamma and Map3k4 interactions regulate mouse testis determination via p38 MAPK-mediated control of Sry expression. *Dev Cell* 2012; **23**:1020–1031.
10. Warr N, Siggers P, Carre GA, Bogani D, Brixey R, Akiyoshi M, Tachibana M, Teboul L, Wells S, Sanderson J, Greenfield A. Transgenic expression of Map3k4 rescues T-associated sex reversal (Tas) in mice. *Hum Mol Genet* 2014; **23**:3035–3044.
11. Warr N, Siggers P, Carre GA, Wells S, Greenfield A. Genetic analyses reveal functions for MAP2K3 and MAP2K6 in mouse testis determination. *Biol Reprod* 2016; **94**:103.
12. Cuevas BD, Abell AN, Johnson GL. Role of mitogen-activated protein kinase kinase kinases in signal integration. *Oncogene* 2007; **26**:3159–3171.
13. Gerwins P, Blank JL, Johnson GL. Cloning of a novel mitogen-activated protein kinase kinase kinase, MEKK4, that selectively regulates the c-Jun amino terminal kinase pathway. *J Biol Chem* 1997; **272**:8288–8295.
14. Abell AN, Johnson GL. MEKK4 is an effector of the embryonic TRAF4 for JNK activation. *J Biol Chem* 2005; **280**:35793–35796.
15. Abell AN, Rivera-Perez JA, Cuevas BD, Uhlik MT, Sather S, Johnson NL, Minton SK, Lauder JM, Winter-Vann AM, Nakamura K, Magnuson T, Vaillancourt RR et al. Ablation of MEKK4 kinase activity causes neurulation and skeletal patterning defects in the mouse embryo. *Mol Cell Biol* 2005; **25**:8948–8959.
16. Bullejos M, Koopman P. Delayed Sry and Sox9 expression in developing mouse gonads underlies B6-Y(DOM) sex reversal. *Dev Biol* 2005; **278**:473–481.
17. Bouma GJ, Washburn LL, Albrecht KH, Eicher EM. Correct dosage of Fog2 and Gata4 transcription factors is critical for fetal testis development in mice. *Proc Natl Acad Sci U S A* 2007; **104**:14994–14999.
18. Abell AN, Granger DA, Johnson GL. MEKK4 stimulation of p38 and JNK activity is negatively regulated by GSK3beta. *J Biol Chem* 2007; **282**:30476–30484.
19. Mobley RJ, Raghu D, Duke LD, Abell-Hart K, Zawistowski JS, Lutz K, Gomez SM, Roy S, Homayouni R, Johnson GL, Abell AN. MAP3K4 controls the chromatin modifier HDAC6 during trophoblast stem cell epithelial-to-mesenchymal transition. *Cell Rep* 2017; **18**: 2387–2400.
20. Li Y, Taketo T, Lau YF. Isolation of fetal gonads from embryos of timed-pregnant mice for morphological and molecular studies. *Methods Mol Biol* 2012; **825**:3–16.
21. Warr N, Siggers P, Bogani D, Brixey R, Pastorelli L, Yates L, Dean CH, Wells S, Satoh W, Shimono A, Greenfield A. Sfrp1 and Sfrp2 are required for normal male sexual development in mice. *Dev Biol* 2009; **326**:273–284.
22. Abell AN, Granger DA, Johnson NL, Vincent-Jordan N, Dibble CF, Johnson GL. Trophoblast stem cell maintenance by fibroblast growth factor 4 requires MEKK4 activation of Jun N-terminal kinase. *Mol Cell Biol* 2009; **29**:2748–2761.
23. Raghu D, Mobley RJ, Shendy NAM, Perry CH, Abell AN. GALNT3 maintains the epithelial state in trophoblast stem cells. *Cell Rep* 2019; **26**:3684–3697 e7.
24. Kim Y, Capel B. Balancing the bipotential gonad between alternative organ fates: a new perspective on an old problem. *Dev Dyn* 2006; **235**:2292–2300.
25. Kim Y, Kobayashi A, Sekido R, DiNapoli L, Brennan J, Chaboissier MC, Poulat F, Behringer RR, Lovell-Badge R, Capel B. Fgf9 and Wnt4 act as antagonistic signals to regulate mammalian sex determination. *PLoS Biol* 2006; **4**:e187.
26. Jorgensen JS, Gao L. Irx3 is differentially up-regulated in female gonads during sex determination. *Gene Expr Patterns* 2005; **5**: 756–762.
27. Small CL, Shima JE, Uzumcu M, Skinner MK, Griswold MD. Profiling gene expression during the differentiation and

development of the murine embryonic gonad. *Biol Reprod* 2005; **72**: 492–501.

28. Aissouni Y, Zapart G, Iovanna JL, Dikic I, Soubeyran P. CIN85 regulates the ability of MEKK4 to activate the p38 MAP kinase pathway. *Biochem Biophys Res Commun* 2005; **338**:808–814.
29. Wong CK, Luo W, Deng Y, Zou H, Ye Z, Lin SC. The DIX domain protein coiled-coil-DIX1 inhibits c-Jun N-terminal kinase activation by Axin and dishevelled through distinct mechanisms. *J Biol Chem* 2004; **279**:39366–39373.
30. Miyake Z, Takekawa M, Ge Q, Saito H. Activation of MTK1/MEKK4 by GADD45 through induced N-C dissociation and dimerization-mediated trans autophosphorylation of the MTK1 kinase domain. *Mol Cell Biol* 2007; **27**:2765–2776.
31. Takekawa M, Saito H. A family of stress-inducible GADD45-like proteins mediate activation of the stress-responsive MTK1/MEKK4 MAPKKK. *Cell* 1998; **95**:521–530.
32. Eicher EM, Washburn LL, Schork NJ, Lee BK, Shown EP, Xu X, Dredge RD, Pringle MJ, Page DC. Sex-determining genes on mouse autosomes identified by linkage analysis of C57BL/6J-YPOS sex reversal. *Nat Genet* 1996; **14**:206–209.
33. Eicher EM, Washburn LL, Whitney JB 3rd, Morrow KE. Mus poschiavinus Y chromosome in the C57BL/6J murine genome causes sex reversal. *Science* 1982; **217**:535–537.
34. Whitney JB, Mills TM, Lewis RW, Wartell R, Abney TO. A single genetic determinant that prevents sex reversal in C57BL-YPOS congenic mice. *Biochem Genet* 2000; **38**:119–137.
35. Washburn LL, Eicher EM. Sex reversal in XY mice caused by dominant mutation on chromosome 17. *Nature* 1983; **303**:338–340.
36. Washburn LL, Eicher EM. Normal testis determination in the mouse depends on genetic interaction of a locus on chromosome 17 and the Y chromosome. *Genetics* 1989; **123**:173–179.
37. Washburn LL, Lee BK, Eicher EM. Inheritance of T-associated sex reversal in mice. *Genet Res* 1990; **56**:185–191.
38. Carre GA, Siggers P, Xipolita M, Brindle P, Lutz B, Wells S, Greenfield A. Loss of p300 and CBP disrupts histone acetylation at the mouse Sry promoter and causes XY gonadal sex reversal. *Hum Mol Genet* 2018; **27**:190–198.
39. Abell AN, Jordan NV, Huang W, Prat A, Midland AA, Johnson NL, Granger DA, Mieczkowski PA, Perou CM, Gomez SM, Li L, Johnson GL. MAP3K4/CBP-regulated H2B acetylation controls epithelial-mesenchymal transition in trophoblast stem cells. *Cell Stem Cell* 2011; **8**:525–537.
40. Shendy NAM, Raghu D, Roy S, Perry CH, Safi A, Branco MR, Homayouni R, Abell AN. Coordinated regulation of Rel expression by MAP3K4, CBP, and HDAC6 controls phenotypic switching. *Commun Biol* 2020; **3**:475.